# Simulation of organ pipe transfer function by means of various numerical techniques

**P. Rucz** [1], **J. Angster**[2], **F. Augusztinovicz** [1], **P. Fiala** [1], **A. Miklós**[2], **N. M. Ortiz**[2]
[1] Budapest University of Technology and Economics,
Department of Telecommunications, Laboratory of Acoustics
Magyar Tudósok körútja 2., H-1117 Budapest, Hungary
e-mail: **rucz@hit.bme.hu**

[2] Fraunhofer Institute for Building Physics,
Group of Musical Acoustics and Photoacoustics
Nobelstrasse 12, D-70569 Stuttgart, Germany

## Abstract

Designing and manufacturing processes of organ pipes are still based on traditional prototyping methods and applying step-by-step tuning and voicing adjustments. To speed up this rather time and resource consuming procedure, a modeling approach is being developed. To be able to simulate complex physical phenomena of the sound generation process, a number of pipe models have already been set up by several researchers and scientists. In general, these models treat the pipe resonator as a simple one-dimensional system, described by approximative analytical formulas. Contrary to this, the present paper examines numerical acoustical models for the pipe resonator. The performance and accuracy of three different simulation technique is tested, involving the usage of self-developed and commercial software packages. Real prototype pipes are modeled by the boundary element, coupled finite / boundary element and finite / infinite element methods. The results are compared to each other and measurement data. Possibilities of expanding the model by non-acoustical parts is also examined.

## 1 Introduction

Scaling of organ pipes is still performed according to rules that were laid down in the 19th century. These rules prescribe pipe dimensions and setup of tuning devices for the desired tone, but in some cases changing the traditional geometry parameters is inevitable for aesthetic or practical reasons. Then the organ builder can rely only on his experience when attempting to tune the sound characteristics of the pipe. The aim of applying computer simulation for organ pipe acoustics is twofold. On one hand, it can provide scientific basis for dimensioning the pipes and tuning devices, such as tuning slides, rolls and openings. On the other hand, its application will hopefully help speeding up the manufacture processes of scaling and tuning.

In spite of the simplicity of the pipe geometry, setting up a realistic model for the sound production is not straightforward, because the sound generation mechanism is a complex physical process. It involves acoustical, vibrational and fluid flow phenomena inherently and nonlinearly coupled. This process has already been investigated for over one and half century by many researchers, and is still an active field of research in both musical acoustics and fluid dynamics. Various models, experiments and results have been presented in a great number of papers, books and other publications.

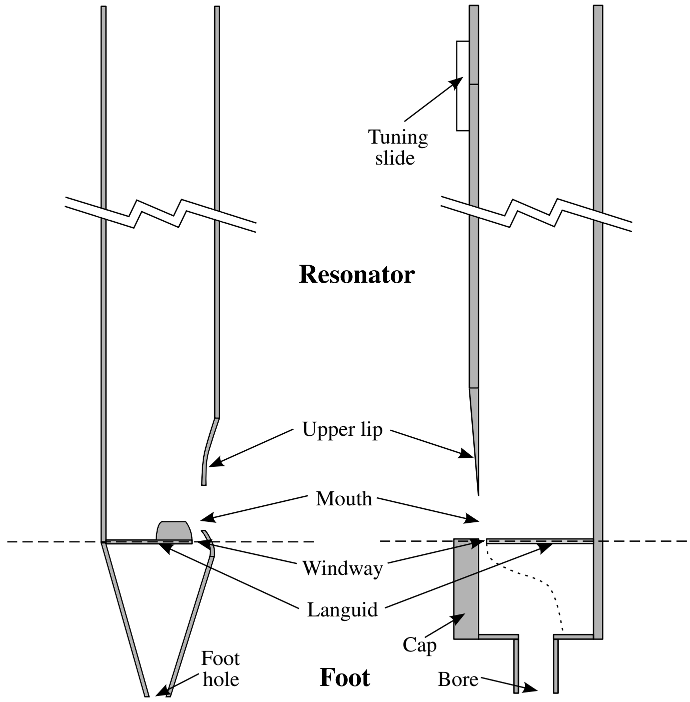


Figure 1: Longitudinal sections of a cylindric metal (left) and a rectangular wooden (right) labial organ pipe

The approach, that is presented herein, is also based on the the separation of the complex mechanism, like the models of Fletcher [1, 2], McIntrye et al. [3], Verge et al. [4] or Adachi [5]. Different from previous models, in which the linear acoustic parts are treated in much more simple ways than other phenomena, the present examination is focused merely on the acoustic parts of the complete system. These parts are represented by the pipe resonator, whose behavior is described by its transfer function. The pipe transfer function plays a key role in forming the characteristics of the steady state sound, therefore important parameters of the pipe sound can be predicted from it. Our computations are carried out in the frequency domain, thus transient attacks will not be analyzed. There are various, both analytical and numerical methods that are capable of solving this simplified, air cavity problem. The aim of this paper is to examine these techniques and compare them in accuracy, efficiency and the ability of being extended by mechanical and air flow parts.

# 2 The pipe sound and the transfer function

## 2.1 The sound generation mechanism

Figure 1 shows longitudinal sections of two typical types of flue organ pipes. As the player presses the corresponding key on the keyboard a valve is opened, which lets air flow into the pipe. When the flowing air enters the pipe foot through the foot hole (or bore) the pressure is increased in the foot part. Air starts to flow through the windway forming a thin jet. This jet hits the upper lip of the pipe and generates the so called edge tone which provides the excitation of the air column resonating inside the pipe body. Because of the physical coupling between the jet excitation and the acoustic wave propagation inside the resonator part, the air jet starts to oscillate around the upper lip and its periodic movement is maintained during the steady state sound generation.

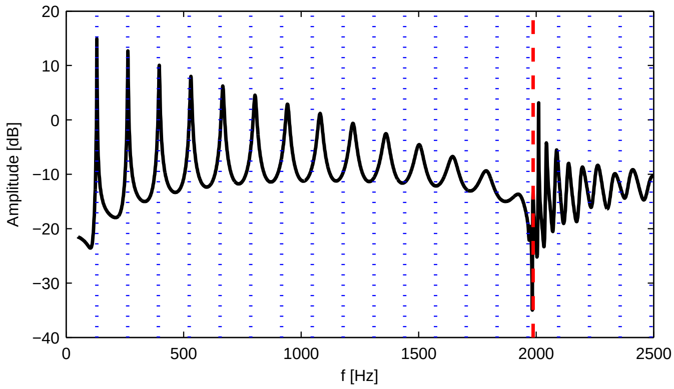


Figure 2: Typical pipe transfer function of an open flue organ pipe — Pipe transfer function ··· Exact harmonics of the fundamental −− Cut-off frequency

## 2.2 Properties of the pipe transfer function

Due to the periodic excitation signal, harmonic lines are seen in the sound spectrum. The resonator part can amplify or depress these spectral components, forming the steady state sound spectrum of the pipe. This effect is described by the transfer function of the pipe, which is determined by the geometry of the resonator and the openings (mouth, open end and tuning openings). Thus, the resonator's transfer function has a great influence on the sound characteristics of the pipe. A typical pipe transfer function is shown in figure 2. The most important characteristic properties of the pipe transfer function are the following.

- Fundamental frequency

  The first resonant frequency of the air column inside the resonator. In most cases, this is also the musical tone of the pipe, however, voicing settings and overblowing can change this situation. Even though, other harmonics can dominate in the attack transient, usually the fundamental component has the greatest amplitude in the steady state sound.

- Frequencies of further modes

  As it is seen in figure 2, further modes are not exact harmonics of the fundamental, they are slightly stretched in frequency. This phenomenon, whose effect is highly dependent on the geometry of the resonator, is called stretching, and this is a very characteristic feature of the transfer function. The stretching factors are calculated simply by dividing the frequency of the $n^{\text{th}}$ mode by the fundamental frequency:

$$\text{Stretch}_{\text{n}} = \frac{f_n}{f_1}. \tag{1}$$

  The stretching effect can be understood by taking into consideration the frequency dependency of the radiation impedances at the openings, or the end correction effect, in other words. There are special pipe types with more complex resonator shapes and pipe transfer functions. In this case, the ratio of the frequencies of pipe modes is not interpreted as stretching, because waveforms in the resonator are no longer purely sinusoidal. A typical example is the chimney pipe, which has a coupled resonator that consists of the pipe body and the chimney attached on its top. Acoustical behavior of chimney pipes is discussed in e.g. [6] and their transfer function is also examined in the present paper.

- Goodness factor of resonances

  The peaks of different modes are not equally sharp, this is due both to radiation impedances and wave propagation losses, namely viscous and thermal effects. The latter are more significant for high frequencies and narrow tubes, therefore the goodness factor is decreasing for successive modes.

- Cut-off frequency

  Since the diameter (or depth for rectangular pipes) is much smaller than the length of the resonator, pure longitudinal modes appear at low frequencies. The frequency, where transversal modes start to appear, is called cut-off frequency. Because of the excitation of mixed modes, the transfer function shows irregularities from this point on, as it is seen in figure 2.

In spite of the fact, that the pipe transfer function has a huge influence on the steady state characteristics, there are a number of effects in the organ sound (such as transients), which cannot be described merely by the transfer function. To tune the speech of the pipes organ voicers apply two different processes. In the voicing process, the excitation parameters (properties of the air jet and pressure level in the pipe foot) are set up and fine tuned; whereas the tuning process consists of pipe scaling setting up tuning devices. The latter is of the utmost importance in forming the pipe transfer function.

# 3 Methods of the solution

## 3.1 Analytical approach

Since the geometry of organ pipe resonators is not too complex usually, it is reasonable to use a one-dimensional analytical model of the pipe. This model consists of an acoustic duct complemented by radiation impedance models attached to the openings of the pipe. The behavior of the resonator is determined by the input impedance function. Tor closed pipes resonances occur at frequencies, where the input impedance has local maximum, while open pipes resonate at frequencies of minimal input impedance (maximal input admittance). The input impedance of an acoustic duct of length $L$ is given as:

$$Z_{\mathrm{P}} = Z_0 \frac{Z_{\mathrm{R}} + \mathrm{j} Z_0 \tan kL}{Z_0 + \mathrm{j} Z_{\mathrm{R}} \tan kL}, \tag{2}$$

where j denotes the imaginary unit, $Z_{\mathrm{R}}$ symbolizes the radiation impedance and $Z_0 = \varrho_0 c$ stands for the plane wave impedance, with $\varrho_0$ being the average density of air and $c$ the speed of sound. Radiation impedance models for the open end and the mouth opening, that are used in our analytical calculations are examined in more details in [7] or [8].

Despite of its simplicity, the one-dimensional model generally provides a good approximation under the cut-off frequency. It should be noted that this method can only be applied to pipes with simple and regular geometry.

## 3.2 The indirect Boundary Element Method

The indirect boundary element method (IBEM) is capable of solving the internal and external acoustical radiation and scattering problems simultaneously. The geometry model for this technique is a surface mesh with perfectly rigid and infinitely thin walls. Zero pressure jump boundary conditions are applied at free edges of the mesh to ensure the continuity and smoothness of the sound field. The discretization process of this method leads to systems of algebraic linear equations with full and frequency dependent system matrices. Thus, the system matrices have to be assembled for every distinct testing frequency and fast matrix inversion techniques can not be applied on them because of their fullness. On the other hand, the complexity rises proportional to the second power of the resolution, as we have a surface mesh. A field point mesh can be set up to visualize the waveform inside or near the resonator. IBEM simulations are run using the SYSNOISE commercial software package.

### 3.3 The coupled Finite / Boundary Element Method

Another approach of modeling is to build up the air cavity with finite elements and apply the direct boundary element method to set up boundary conditions. Two types of boundary conditions are set up: at pipe walls the normal particle velocity is set to zero, while at the openings impedance boundary conditions are constructed. Since the area of the openings are much smaller than that of the walls, the impedance matrices can be expressed in Schur complement form to reduce their size. One more technique, that can speed up this process, is to make use of the fact that the boundary conditions are varying smoothly dependent of the frequency, and apply interpolation formulas to obtain the impedance matrices. By doing so, the BEM has to be invoked for only a small number of testing frequencies which means a remarkable reduction of computational effort. The disadvantage compared to the IBEM method is that the complexity rises with the third power of the resolution as a volume mesh of the geometry is set up. The set of equations that are to be solved is described by mainly sparse and frequency independent system matrices, complemented by the much smaller, frequency dependent and full impedance matrix. This technique is implemented in a self-developed piece of software in MATLAB.

Alternatively, it would also be possible to create a finite element mesh and set up boundary conditions from analytical approximations. This method was presented in [9] and provided unacceptably inaccurate results, therefore it is not examined herein.

### 3.4 Finite Element Method with Infinite elements

An alternative model can be set up by extending the finite element computational domain by parts that are outside of the pipe, forming a convex circumscribing shape. Then, by means of the Atkinson–Wilcox theorem local boundary conditions can be applied on the convex boundary instead of global boundary conditions incorporated by the BEM. The infinite element method is one technique to form these local boundary conditions. This leads to frequency independent, sparse system matrices, which means that the solution for the equations can be carried out much faster. However, the degrees of freedom are increased because of the extension of the computational domain and the additional infinite elements. The complexity grows proportional to the third power of the resolution because a volume mesh is used. The waveforms in the acoustic field are obtained straightforwardly from the solution. The IEM technique was implemented in a self-developed software package in MATLAB.

The most important properties of the three applied numerical techniques are summarized in table 1.

| Technique | Mesh type | Frequency dependency of system matrices | Density of system matrices | Extra DOFs |
|---|---|---|---|---|
| Indirect BEM | Surface | Fully dependent | Full | No |
| Coupled FEM/BEM | Volume | Partially dependent | Sparse with full coupling matrix | No |
| FEM/IEM | Volume | Not dependent | Sparse | Yes |

Table 1: Comparison of most important properties of numerical techniques applied for pipe transfer function simulation.

## 4 Measurement and simulation setup

### 4.1 Setup for the pipe transfer function measurement

The setup for organ pipe transfer function measurements is shown in figure 3. In contrast to the sound generation mechanism, the excitation is provided by an external source, which is placed in the longitudinal

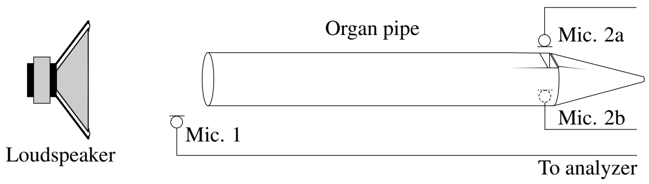


Figure 3: Setup for organ pipe transfer function measurements

axis of the pipe. Thus, the resonator is examined as an individual acoustical system, separated from the other parts of the pipe.

The excitation signal can be a broadband signal, like a periodic chirp or a swept/stepped sine. Microphone 1 is located near the open end of the pipe, and its signal serves as a reference for correcting the amplitude characteristics of the sound source. Microphone 2 is placed inside the pipe, near the languid, opposite to the mouth. If this can not be done, the microphone can also be placed near the mouth opening. The signals received by the microphones are connected to a two channel FFT analyzer, which calculates the transfer function. The whole setup is assembled inside an anechoic chamber, that provides the properties of a free sound field. The measurements presented in this paper were carried out in the anechoic chamber of the Fraunhofer Institute for Building Physics, Stuttgart.

### 4.2 Simulation settings

Simulation setups model the arrangement of transfer function measurements. The loudspeaker is represented by an ideal point source, that radiates with unit amplitude at every distinct testing frequency. The microphones are represented by simple field points and the frequency response of the field point corresponding to the location of microphone 2 gives the transfer function. Extra field points can be set up in order to display waveforms of the sound field.

Model geometries are generated using an algorithm that creates symmetrical meshes with quad surface and hexa volume elements. The mesh resolution is set corresponding to the measured cut-off frequencies of the pipes, following the thumb role of at least eight elements per wavelength for the maximal testing frequency. Testing frequencies are chosen uniformly in the range from 50 Hz to 2.5 kHz with 1 Hz steps. This frequency range covers the fundamental and several longitudinal modes for all of the tested pipe models.

## 5 Experiments and results

Two different types of open labial organ pipes were examined in the course work that is reported herein: standard rectangular wooden pipes and cylindric metal chimney pipes. These pipe types have clearly distinguishable sound characteristics because of their completely different resonator shape. In the following sections computational results and measurement data are compared for a few prototype pipes of both types.

The most important properties of numerical pipe models are displayed in tables 3 and 5. It is seen, that contrary to the small number of DOFs in the IBEM model, fullness of the system matrix yields a system of equations whose solution can be more expensive computationally than the same for other methods.

The coupled FE/BE method provides low number of DOFs and also low number of non-zero elements in the system matrix. However, it should be noted, that generation of the coupling impedance matrix in its Schur complement form requires the solution of BEM equations. As it was described in section 3, interpolation formulas can remarkably reduce the computational time spent on calculating the frequency dependent coupling matrix. Nevertheless, our experiments have shown that the evaluation of BEM equations remains a

| Pipe | Length | Width | Depth | Mouth height | Mouth width |
|---|---|---|---|---|---|
| 4/16 | 1180 | 69.80 | 86.87 | 19.87 | 68.64 |
| 4/18 | 1181 | 61.20 | 98.32 | 21.53 | 60.76 |
| 4/20 | 1179 | 55.34 | 108.40 | 25.34 | 53.93 |

Table 2: Wooden pipe dimensions given in mm.

significant part in the whole computational effort. Properties of each technique (see table 1) are clearly seen in the numerical data of tables 3 and 5.

As numerical techniques are implemented in different environments, the exact quantitative comparison of computational times can not be performed. Qualitative comparison of computational efforts has shown that simulation times for the three methods are of the same order of magnitude, if geometry meshes of the same resolution are used. From this point of view, it can be assessed that neither of these techniques performs significantly better or worse comparing one to another. Thus, the performance of the methods is to be compared based solely on the accuracy of results in the following section, using measurement data as a point of reference.

The quantities that are compared are the frequencies of the first few longitudinal modes and their corresponding ratios to the frequency of the first mode (fundamental). Goodness factors of resonances are not compared herein, as simulation techniques in this form lack the ability of modeling air (viscous) and wall (thermal) losses. Therefore, simulation gives remarkably higher goodness factors, especially at higher frequencies where losses are more significant. Qualitatively, it is seen (figures 4 and 5), that successive modes have decreasing goodness factors, as it is expected because of the frequency dependency of radiation impedances. In spite of the fact, that the examined quantities do not characterize the steady state pipe sound completely, these are the most important parameters that are finely adjusted during the scaling and tuning processes.

## 5.1 Wooden pipe experiments

Wooden pipe simulations are run on a series of open pipes, which already have been built and measured at the Fraunhofer Institute in Stuttgart. These pipes were designed as a part of an experiment that examined the effects of scaling on the sound characteristics of wooden pipes. Thus, these pipes have different geometrical parameters and similar steady sound characteristics, being appropriate subjects for test simulations. The series consisted of five pipes of C3 tone, three of these were chosen and made simulation models of. Exact dimensions of the pipes are given in table 2. Note: fractions in pipe names refer to mouth width to circumference ratio. Geometry data are found in [10], where the whole experiment is also described in detail.

Properties of numerical wooden pipe models are summarized in table 3. Because of the oblong geometry, the extension of the computational domain, that is required by the FE/IE method, causes a significant increase in the number of DOFs. As it can be seen, the FE/IE method gives a model with even 20–25 times more DOFs than the IBEM model, and 12–16 times more than the coupled method. On the other hand, sparsity of the system matrices lead to a system of equations half or one third as complex as the IBEM equations.

Transfer function of pipe 4/16 is shown in the left hand side of figure 4. The effect of stretching and decreasing goodness factors of successive modes are clearly seen. Irregularities due to transversal modes appear near 2 kHz, which is in good correspondence with the measured cut-off frequency of 1987 Hz. The right hand side of figure 4 displays the sinusoidal waveforms in the longitudinal section of the pipe. It is seen that near the mouth opening, the one dimensional approximation of analytical models is no longer valid.

Comparison of wooden pipe results is shown in table 6. Frequencies and stretching factors of the first five modes are compared. The IBEM technique gives the best approximation for the fundamental frequencies with relative errors of around 1 %. The coupled and the FE/IE methods predict the frequency of the first

| Technique | Pipe | DOF | Non-zero elements |
|---|---|---|---|
| Indirect BEM | 4/16 | 1 294 | 1 674 436 |
| | 4/18 | 1 437 | 2 064 469 |
| | 4/20 | 1 580 | 2 496 400 |
| Coupled FEM/BEM | 4/16 | 2 100 | 45 289 |
| | 4/18 | 2 450 | 53 876 |
| | 4/20 | 2 760 | 61 655 |
| FEM/IEM | 4/16 | 33 872 | 810 484 |
| | 4/18 | 35 448 | 848 776 |
| | 4/20 | 35 720 | 853 684 |

Table 3: Comparison of properties of applied numerical models for wooden pipes.

model with 3–4% relative errors, which means they perform more poorly than the analytical relations. Frequencies of the 2$^{nd}$ to 5$^{th}$ modes are also determined most accurately by the IBEM method. In case of pipes 4/16 and 4/18 the coupled method gives a significant error for the second mode, which results of a stretching factor that is smaller than 2. This phenomenon is not observed for pipe 4/20.

Stretching factors of the 3$^{rd}$ to 5$^{th}$ modes are calculated with the less error by the FE/IE method. While the analytical technique and the IBEM underestimates the measured values, the FE/IE method gives a slight overestimation.

### 5.2 Chimney pipe experiments

Chimney pipe measurements were carried out on prototype pipes with adjustable resonator and chimney lengths. Three experiments with slightly different setups of pipe dimensions are selected to be reported herein. Exact dimension settings are given in table 4. The chimney length is set to 240 mm in all cases and the resonator length is varied in 20 mm steps.

Properties of numerical chimney pipe models are shown in table 5. For chimney pipes, the the difference between the number of DOFs is greater between the IBEM and FEM/BEM models and smaller between the coupled and FEM/IEM models. While the number of DOFs increased for the IBEM and coupled methods compared to wooden pipes, the extension of the computational domain for the FEM/IEM method leads to smaller number of DOFs this time. While the number of DOFs in the FE/IE model is 15 times higher, the number of non-zero elements in the system matrix is five time less compared to the IBEM model. The relation between the number of DOFs and non-zero elements in the system matrix is similar to the case of wooden pipes for all three methods.

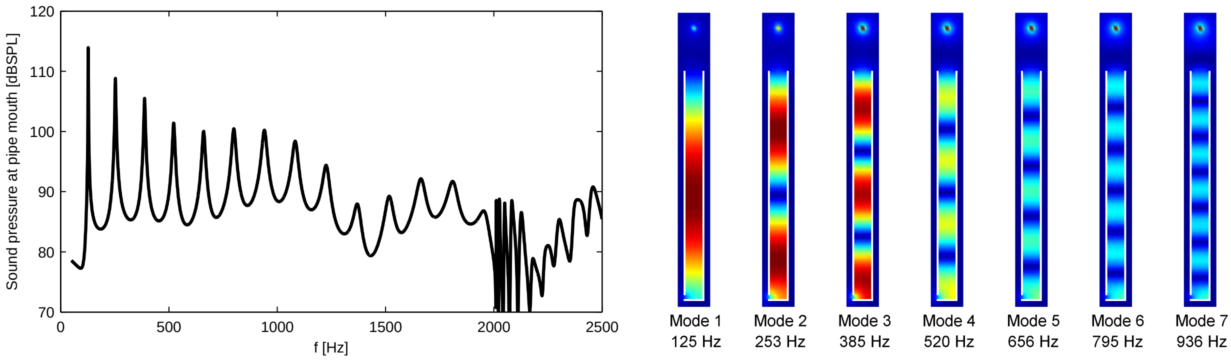


Figure 4: Simulated transfer function (left) and longitudinal modes (right) of chimney pipe N265. Result of coupled FEM/BEM and FEM/IEM simulations.

| Pipe / Property | N265 | N065 | P135 |
|---|---|---|---|
| Resonator length | 576.00 | 596.00 | 616.00 |
| Resonator diameter | 79.00 | | |
| Chimney length | 240.00 | | |
| Chimney diameter | 28.72 | | |
| Mouth height | 25.66 | | |
| Mouth width | 59.99 | | |

Table 4: Chimney pipe dimensions given in mm.

| Technique | Pipe | DOF | Non-zero elements |
|---|---|---|---|
| Indirect BEM | N265 | 1 796 | 3 225 616 |
| | N065 | 1 832 | 3 356 224 |
| | P135 | 1 868 | 3 489 424 |
| Coupled FEM/BEM | N265 | 5 552 | 132 956 |
| | N065 | 5 792 | 138 668 |
| | P135 | 5 912 | 141 524 |
| FEM/IEM | N265 | 26 496 | 623 404 |
| | N065 | 27 200 | 639 628 |
| | P135 | 27 552 | 647 740 |

Table 5: Comparison of properties of applied numerical models for chimney pipes.

Simulated transfer function of pipe N265 is shown in the left hand side of figure 5. As it is seen the pipe with the attached chimney acts as a coupled resonator and therefore ratios of the frequencies of the modes are irregular. The cut-off is out of the frequency range of the simulation for these pipes, hence this effect is not seen on the diagram. The waveforms belonging to the first seven longitudinal modes are displayed in the right hand side of figure 5. Modes 3, 4 and 7 show the role of the chimney and the coupled resonator behavior.

Table 7 shows measurement and simulation data for the three chimney pipe models. Frequencies and ratios to the fundamental for the first five longitudinal modes are given. Contrary to wooden pipe results, for fundamental frequencies of chimney pipes, coupled and FEM/IEM models give more precise results than the analytical approximations and the IBEM. All the applied techniques predict the fundamental within the relative error range of 1.5%. For higher number modes, the coupled technique gives the most accurate results in most cases. Relative errors are under 3% for all the methods, which is a good result, considering

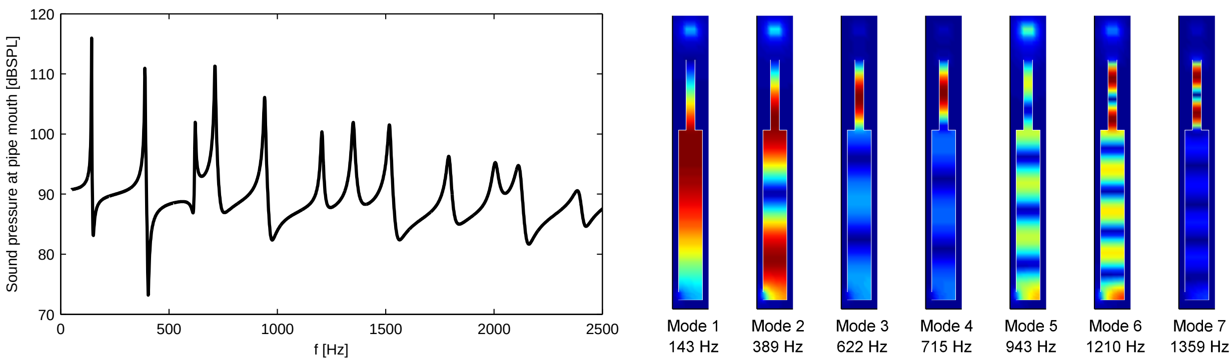


Figure 5: Simulated transfer function (left) and longitudinal modes (right) of chimney pipe N265. Modes 3, 4 and 7 show the role of the chimney in forming the transfer function of the pipe. Result of IBEM and FEM/IEM simulations.

the simplicity of the model.

Pipe dimensions have a great influence on forming the transfer function of chimney pipes. With the proper selection of the dimensions, a chosen harmonic can be amplified in the pipe sound. Using simulation results, optimal pipe dimensions can be found for the desired amplification of a certain harmonic. Results related to this issue are yet to be presented in another publication.

### 5.3 Model improvement

All the three applied numerical techniques are based on a linear acoustical approach and no other phenomena is included in the models. However, even the pipe transfer function is affected by viscous and thermal losses, that can be of the same order of magnitude as losses due to radiation impedances at high frequencies [11]. The modeling of these effects would require a damping model of air or a boundary layer simulation. A finite element model is capable of incorporating parts of these kind, even if a boundary layer simulation would require a much higher resolution near the pipe walls. The boundary element method is more inflexible in this aspect.

Simulation of wall vibrations would be possible using a coupled mechanical–acoustical finite or boundary element method. Wooden pipes mean a challenge in these models because of the anisotropic behavior of the material.

The most complex element in the sound generation is the excitation mechanism. Precise modeling of the edge tone and the interaction between acoustic and fluid flow parts would require a coupled CFD and acoustic model with high resolution. An excitation model based on fluid flow simulation can be adjoint to a finite element model, both the coupled FE/BE and FE/IE methods can be used for this.

## 6 Summary and conclusions

A numerical approach for modeling resonator parts of labial organ pipes is presented in this paper. Three essentially different techniques are applied to model open wooden and metal chimney pipes. Impedance analysis and examination of the end-correction effect shows good fit to approximative analytical calculations. Modeling of real prototype pipes and comparison to transfer function measurements show, that the three applied techniques are capable of simulating the pipe resonator and can perform better than analytical models in certain cases. Neither of the methods performed significantly better or worse than the other two, regarding computational effort and accuracy compared to measured values. Three dimensional numerical models provide a way to simulation of irregular geometries, where analytical approximations can not be used. However, this particular property has not yet been tested on real pipe models.

This paper focuses on merely acoustical phenomena, nevertheless, it was seen that to take into account complex processes of the sound generation mechanism and losses due to viscosity and thermal interaction in the resonator, a more complex model is needed. Modeling wall losses would enable the goodness factor analysis of pipe modes, whereas a fluid flow model of the excitation mechanism would make possible the simulation of transient attacks. The extension of the model by loss simulation, fluid flow and mechanical parts and are the authors' future plans.

## Acknowledgments

This research is supported by the European Commission (Research for SMEs, Contract No: 222104) and by 10 European organ builder firms. The authors thank Dr. Seiji Adachi for his valuable contribution and helpful remarks to this paper.

| 4/16 | Measurement | | Analytical | | Indirect BEM | | Coupled FEM/BEM | | FEM/IEM | |
|---|---|---|---|---|---|---|---|---|---|---|
| Mode | F [Hz] | Stretch | F [Hz] | Stretch | F [Hz] | Stretch | F [Hz] | Stretch | F [Hz] | Stretch |
| 1st | 129.9 | 1.000 | 129 | 1.000 | 131 | 1.000 | 128 | 1.000 | 126 | 1.000 |
| 2nd | 261.8 | 2.016 | 259 | 2.008 | 263 | 2.008 | 253 | 1.977 | 255 | 2.024 |
| 3rd | 396.5 | 3.053 | 391 | 3.031 | 397 | 3.031 | 388 | 3.031 | 387 | 3.071 |
| 4th | 537.0 | 4.135 | 527 | 4.085 | 531 | 4.053 | 522 | 4.078 | 521 | 4.135 |
| 5th | 677.6 | 5.218 | 665 | 5.155 | 667 | 5.092 | 660 | 5.156 | 658 | 5.222 |

| 4/18 | Measurement | | Analytical | | Indirect BEM | | Coupled FEM/BEM | | FEM/IEM | |
|---|---|---|---|---|---|---|---|---|---|---|
| Mode | F [Hz] | Stretch | F [Hz] | Stretch | F [Hz] | Stretch | F [Hz] | Stretch | F [Hz] | Stretch |
| 1st | 131.2 | 1.000 | 128 | 1.000 | 130 | 1.000 | 128 | 1.000 | 125 | 1.000 |
| 2nd | 262.4 | 2.000 | 258 | 2.016 | 262 | 2.008 | 252 | 1.969 | 253 | 2.024 |
| 3rd | 400.4 | 3.051 | 391 | 3.055 | 394 | 3.025 | 387 | 3.023 | 384 | 3.072 |
| 4th | 547.1 | 4.169 | 526 | 4.109 | 529 | 4.056 | 521 | 4.070 | 519 | 4.152 |
| 5th | 681.0 | 5.190 | 663 | 5.180 | 664 | 5.095 | 660 | 5.156 | 655 | 5.240 |

| 4/20 | Measurement | | Analytical | | Indirect BEM | | Coupled FEM/BEM | | FEM/IEM | |
|---|---|---|---|---|---|---|---|---|---|---|
| Mode | F [Hz] | Stretch | F [Hz] | Stretch | F [Hz] | Stretch | F [Hz] | Stretch | F [Hz] | Stretch |
| 1st | 131.2 | 1.000 | 129 | 1.000 | 130 | 1.000 | 126 | 1.000 | 125 | 1.000 |
| 2nd | 265.1 | 2.020 | 259 | 2.008 | 262 | 2.007 | 255 | 2.024 | 253 | 2.024 |
| 3rd | 401.7 | 3.061 | 392 | 3.039 | 395 | 3.024 | 388 | 3.079 | 384 | 3.072 |
| 4th | 543.7 | 4.143 | 527 | 4.085 | 529 | 4.053 | 524 | 4.159 | 519 | 4.152 |
| 5th | 679.6 | 5.190 | 667 | 5.171 | 665 | 5.095 | 662 | 5.254 | 656 | 5.248 |

Table 6: Comparison of measurement and calculation results for wooden pipes.

| N265 | Measurement | | Analytical | | Indirect BEM | | Coupled FEM/BEM | | FEM/IEM | |
|---|---|---|---|---|---|---|---|---|---|---|
| Mode | F [Hz] | Ratio | F [Hz] | Ratio | F [Hz] | Ratio | F [Hz] | Ratio | F [Hz] | Ratio |
| 1st | 144.1 | 1.000 | 142 | 1.000 | 143 | 1.000 | 144 | 1.000 | 143 | 1.000 |
| 2nd | 383.6 | 2.662 | 389 | 2.739 | 389 | 2.720 | 392 | 2.722 | 389 | 2.720 |
| 3rd | 640.7 | 4.446 | 623 | 4.387 | 621 | 4.343 | 627 | 4.354 | 622 | 4.350 |
| 4th | 722.2 | 5.012 | 719 | 5.063 | 712 | 4.979 | 722 | 5.014 | 715 | 5.000 |
| 5th | 967.2 | 6.712 | 950 | 6.690 | 942 | 6.587 | 946 | 6.569 | 943 | 6.594 |

| N065 | Measurement | | Analytical | | Indirect BEM | | Coupled FEM/BEM | | FEM/IEM | |
|---|---|---|---|---|---|---|---|---|---|---|
| Mode | F [Hz] | Ratio | F [Hz] | Ratio | F [Hz] | Ratio | F [Hz] | Ratio | F [Hz] | Ratio |
| 1st | 140.1 | 1.000 | 139 | 1.000 | 139 | 1.000 | 140 | 1.000 | 139 | 1.000 |
| 2nd | 375.7 | 2.682 | 377 | 2.712 | 378 | 2.719 | 381 | 2.721 | 378 | 2.719 |
| 3rd | 626.4 | 4.471 | 611 | 4.396 | 609 | 4.381 | 614 | 4.386 | 610 | 4.389 |
| 4th | 708.8 | 5.059 | 709 | 5.101 | 703 | 5.058 | 712 | 5.086 | 705 | 5.072 |
| 5th | 936.9 | 6.687 | 922 | 6.633 | 913 | 6.568 | 918 | 6.558 | 915 | 6.583 |

| P135 | Measurement | | Analytical | | Indirect BEM | | Coupled FEM/BEM | | FEM/IEM | |
|---|---|---|---|---|---|---|---|---|---|---|
| Mode | F [Hz] | Ratio | F [Hz] | Ratio | F [Hz] | Ratio | F [Hz] | Ratio | F [Hz] | Ratio |
| 1st | 136.5 | 1.000 | 135 | 1.000 | 135 | 1.000 | 137 | 1.000 | 136 | 1.000 |
| 2nd | 369.5 | 2.707 | 367 | 2.719 | 368 | 2.726 | 370 | 2.701 | 367 | 2.699 |
| 3rd | 608.5 | 4.458 | 597 | 4.422 | 597 | 4.422 | 600 | 4.380 | 597 | 4.390 |
| 4th | 700.9 | 5.135 | 701 | 5.193 | 694 | 5.141 | 704 | 5.139 | 698 | 5.132 |
| 5th | 909.3 | 6.662 | 895 | 6.630 | 887 | 6.570 | 893 | 6.518 | 889 | 6.537 |

Table 7: Comparison of measurement and calculation results for wooden pipes.

## References


[1] N. H. Fletcher. Sound production by organ flue pipes. *Journal of the Acoustical Society of America*, 60:1119–1132, 1976.

[2] N. H. Fletcher and L. M. Douglas. Harmonic generation in organ pipes, recorders, and flutes. *Journal of the Acoustical Society of America*, 68(3):767–771, 1980.

[3] M. E. McIntrye, R. T. Schumacher, and J. Woodhouse. On the oscillations of musical instruments. *Journal of the Acoustical Society of America*, 74(5):1325–1345, 1983.

[4] M. P. Verge, A. Hirschberg, and R. Caussé. Sound production in recorderlike instruments. ii. a simulation model. *Journal of the Acoustical Society of America*, 101(5):2925–2939, 1997.

[5] S. Adachi. Principles of sound production in wind instruments. *Acoustical Science and Technology*, 25(6):400–405, 2004.

[6] S. J. J. M. F. Kokkelmans, M-P. Verge, A. Hirschberg, A. P. J. Wijnands, and R. L. M. Schoffelen. Acoustic behavior of chimney pipes. *Journal of the Acoustical Society of America*, 105:546–551, 1999.

[7] N. H. Fletcher and T. D. Rossing. *The physics of musical instruments*. Springer, 1991.

[8] D. K. Holger, T. A. Wilson, and G. S. Beavers. Fluid mechanics of the edge tone. *Journal of the Acoustical Society of America*, 62(5):1116–1128, 1977.

[9] G. Szoliva. Effect of tuning devices on the sound generation for open labial organ pipes. Master's thesis, Budapest University of Technology and Economics, 2005. In Hungarian.

[10] E. E. Fontestad. Innovative method for the development of optimal scaling of the depth and width of wooden organ pipes. Master's thesis, Universidad Politécnica de Valencia, 2008.

[11] A. Miklós and J. Angster. Properties of the sound of flue organ pipes. *Acustica-Acta Acustica*, 86:611–622, 2000.